FLOW RATE INFLUENCE ON BIOCLOGGING DEVELOPMENT IN POROUS MEDIA

Tatiana Di Calafiori Amancio

tatiana.calafiori@gmail.com

Instituto Superior Técnico, Universidade de Lisboa, Portugal, 2020

1 Abstract

The presence of biofilm is essential for the functioning of the constructed wetlands since it is responsible for the biological processes of removing organic matter and nutrients. However, its exacerbated presence is a serious operational problem. Thus, it is necessary to better understand the factors that influence the growth of the biofilm enabling the clogging of the porous medium. The present work focused solely on the influence of the flow rate. The evaluation of the influence of the flow rate on the development of biofilm in a porous medium occurred through two experiments with different flows (1.9 - 2.0 L/h and 0.9 - 1.0 L/h) in an experimental installation in which three 1.5 L reactors simulated porous media with pores of different sizes (1 mm, 2 mm and 3 mm). Clogging development was measured using a combination of visual and computational methods. The work concluded that for the conditions of the experiments, there is no conclusion about whether the flow influences the development of the bioclogging. Comparing the final absolute values for bioclogging in each reactor, the results showed that the lower flow resulted in thicknesses 30%, 14% and 4% greater than the higher flow for, respectively, 1 mm, 2 mm and 3 mm; however, with standard deviations, the difference becomes negligible. Moreover, the work concludes that there is a dependence on pore size in the development of biofilm.

Key-words: Clogging, biofilm, bioclogging, flow rate, porous medium

2 Introduction

One of the biggest problems in the management of constructed subsurface wetlands with horizontal flow is the clogging of the porous medium through which wastewater treatment occurs. This clogging consists of the occupation of the interstices of the filling medium by solid material that obstructs the passage of wastewater and other materials (Correia 2016). The phenomenon of clogging depends on many factors and on the dynamic relationships between them. One of the possible causes of clogging is the growth of biofilm, also called bioclogging.

Nowadays, bioclogging has become the subject of various studies seeking to better understand its functioning and the factors that affect its growth, although these are not yet definitive and often portray these processes as some kind of black box. For example, in Samsó et al. (2016), the authors take into consideration a uniform development in biofilm thickness that is independent of pore dimensions, which has not been experimentally verified.

One of the main influencers of biofilm development (and inherently of bioclogging) is the flow rate value. On this factor, which is the topic analysed in this work, there are still no precise conclusions, since both biofilm growth and detachment increase at higher flow rate values, due to, on the one hand, the increase in mass transfer that facilitates the transport of nutrients for biofilm growth, and, on the other hand, the increase in the drag force of the medium, causes greater detachment of the biofilm (Liu et al. 2019).

Of all the studies on this subject, Kim et al. (2010) have found that bioclogging at a high flow rate can be accelerated by trapped and accumulated biofilm and can be easily eliminated by high drag force. The authors have also noted that low flow clogging can be delayed by the local biofilm growth time in narrow "pore necks", but the biofilm is rigid enough not to be detached. Araújo et al. (2016) studied the influence of the flow rate, and consequent speed, on the growth of biofilm formed by *Pseudomonas fluorescens* at three different speeds: 0.1 m/s; 0.4 m/s and 0.8 m/s, in which it concluded that an increase in the flow rate promoted a reduction in the thickness of the biofilm, due to the drag stresses, even if the mass of the biofilm remained constant. Thus, an increase in flow velocity results in more compact and denser biofilm. Ostvar et al. (2018) studied the effects of flow rate on biofilm growth in three-dimensional porous media. The results show that the greatest reduction in permeability and porosity was observed in the intermediate flow (0.045 L/h), concluding that in the lower flow the growth of biofilm was affected by the limit of oxygen circulation, and in the higher flow the growth was affected by the entrainment stress. Finally, the experience of (Liu et al. 2019) shows that increased fluid velocity can facilitate biofilm growth, but that above a velocity limit, both biofilm detachment and the inhibition of biofilm formation due to high shear force were observed.

3 Material and Method

The installation used for the work, presented in Figure 3.1 and Figure 3.2, consisted of three reactors, Tupperware-type boxes, independent and submerged in a water bath equipment, which prevented temperature oscillation, as previously developed by (Felício 2018). Each reactor was connected to an aeration chamber and to another chamber for the feeding inlet. This installation was operated during both stages of the study. To prevent algae growth in the reactors, the installation was covered with aluminium foil during the experiments. Each reactor was composed of a simulation of a porous medium composed of five PVC plates arranged vertically and perpendicular to the feeding flow with holes of different diameters (1 mm, 2 mm, or 3 mm).

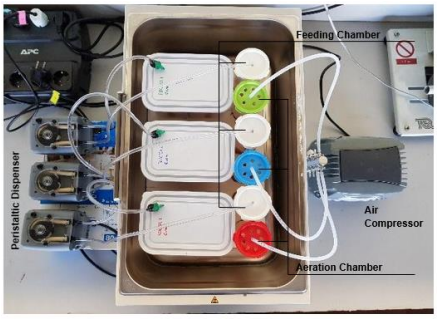

Figure 3.1 - Installation prepared for the first stage (Reactor 1 on top, Reactor 2 in the middle and Reactor 3 below)

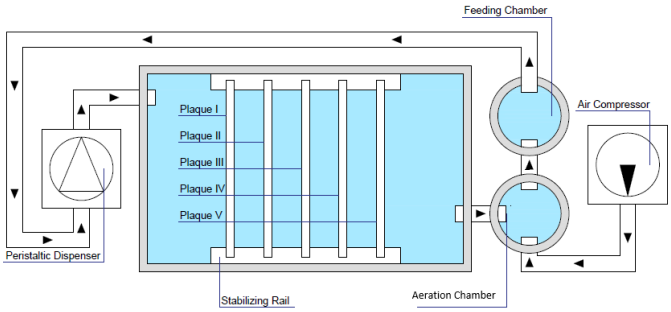

Figure 3.2 - Schematic of a reactor operation (Adapted from (Felício 2018))

The first stage of the experiment began on 25th March of 2019, with a flow between 1,9 – 2,0 L/h and ended on 24th May of 2019. After this stage, the system was washed and sterilized. The second stage began on 3rd June of 2019, with a flow rate of between 0,9 – 1,0 L/h, and ended on 22nd July 2019.

The inoculation of the system occurred in the first two weeks of each experiment. The inoculation fluid, which was used to feed the reactors, consisted of 50% by volume biofilm solution and 50% synthetic sewage. The biofilm solution was obtained by hand washing gravel taken from one of the Constructed Wetlands (CW) in the Environmental Laboratory of Instituto Superior Técnico, added to three litres of distilled water and subsequent filtration to prevent the entry of gravel and other materials. The synthetic sewage solution was composed of sodium

acetate trihydrate (VWR Chemicals) and NPK 4-5-6 liquid fertilizer (Delgarden), both of which were dissolved in running drinking water obtained in the same laboratory (whose origin is the Castelo de Bode Dam). The amount of sodium acetate trihydrate and fertilizer per solution of synthetic sewage was determined by the previous study of Felício (2018), being 1,4311 g of acetate and 25 mL of fertilizer per litre of solution generated. For a fortnight, the inoculation solution was renewed three times a week: on Mondays, Wednesdays, and Fridays. After this period, the inlet solution was only the synthetic sewage solution and the renewal was carried out with the same frequency. At each renewal, pH, temperature, and oxidation-reduction potential (ORP) were measured by means of probes on all the solutions present: the three reactor outlets and the inlet solution.

To monitor the system, TSS and SSV analyses were performed according to existing laboratory standards (APHA-AWWA-WPCF 1995) and COD analyses according to the colorimetric method (5220 D, APHA-AWWA-WPCF 1995) to both output and input solutions. During the weekends, the OD of the reactors was monitored by means of a probe in a feeding chamber of one of the reactors.

To monitor the development of biofilm, five holes of all PVC plates were periodically observed and recorded using a Nikkon SMZ645 stereoscope equipped with a Motic Moticam 10 Mp digital camera, at the Mining Laboratory of Instituto Superior Técnico. For each diameter, the camera software which was used was calibrated to insert the appropriate scale to each photograph according to the magnification used for each hole diameter. To view the entire holes, the 1 mm holes were photographed with a magnification of 4x, the 2 mm holes with a magnification of 2x and the 3 mm holes with a magnification of 1x.

The processing of the photographs was carried out through a programme developed by Felício (2018). The programme first carried out processes to improve the contrast and border definition of the photographs. Then, the program identified the scale of each image. With the scale defined for each photo, the program counted the pixels that had values above (0,51,0) in the RGB system to calculate the area of the unclogged region. Finally, the program returned the processed images, having as white area the unclogged region. As the experiment continued, the number of pixels belonging to the non-clogged region decreased, consequently reducing this area and increasing the area of biofilm clogging. Then the unclogged areas ($A_{non\text{-}clogged}$) were used to calculate the equivalent diameters ($D_{equivalent}$) by means of Equation 3.4. With the temporal evolution of this equivalent diameter it was possible to calculate the variation of the equivalent thickness of the biofilm ($TV_{biofilm}$) which developed and filled the space during the time between the photographs and the respective growth rate (BGR) by means of Equations 3.5 and 3.6. The total biofilm thickness (TBT) on a given day was calculated by the change between the thickness on that day and the thickness on the first day of photography, through Equation 3.7.

$$A_{non-clogged}(mm^2) = {\pi \times D^2_{equivalent}}/{4} \tag{3.4}$$

$$TV_{biofilm}\ (\text{mm}) = {D_{equivalent,ti}(mm) - D_{equivalent,ti+1}(mm)}/{2} \tag{3.5}$$

$$BGR\left(\frac{\text{mm}}{day}\right) = {TV_{biofilm}\ (mm)}/{\Delta t\ (day)} \tag{3.6}$$

$$TBT_{dia\ i}\ (\text{mm}) = {D_{equivalent,ti}(mm) - D_{equivalent,t1}(mm)}/{2} \tag{3.7}$$

4 Results

The first stage, which occurred with a flow rate between 1,9 – 2,0 L/h, presents as main results the evolution of the average unclogged area, the evolution of the biofilm thickness and the biofilm growth rates in each of the three reactors. First, we observe the evolution of the average unclogged area in Figure 4.1.

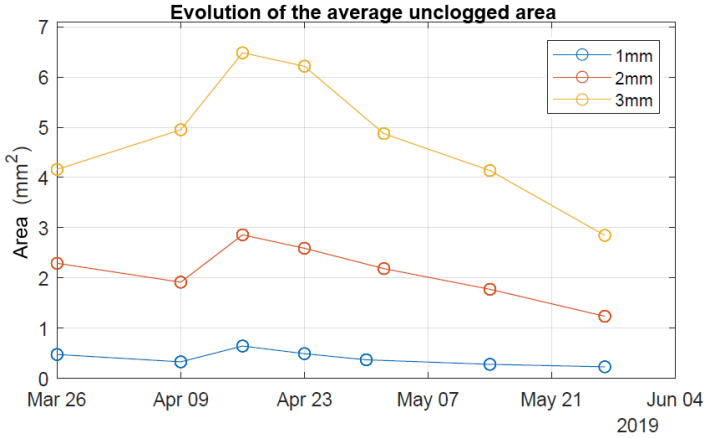

Figure 4.1 - Evolution of the average unclogged area in the first stage

As can be seen, the average unclogged area reaches a maximum on 16th April 2019. This fact occurs due to three factors: (1) the presence of the depth of the plate on the first photo, which decreased the unclogged area calculated in relation to the actual area; (2) the difference in brightness of the day and time that the photos were taken, which resulted in a larger area on a day with less brightness, and (3) a small cleaning of undesirable solids after the first two photos.

From these areas, the evolution of thickness and growth rate was calculated for two different scenarios where the day of zero thickness, which is the value considered to have no biofilm and from this there will be growth of the same, was different. In the first scenario zero thickness was considered on 26th March 2019, and in the second scenario zero thickness was considered on 16th April 2019, ignoring observations from previous days. These two analyses were carried out due to atypical behaviour until the third day, which would originally imply the existence of negative biofilm thickness, which is physically impossible.

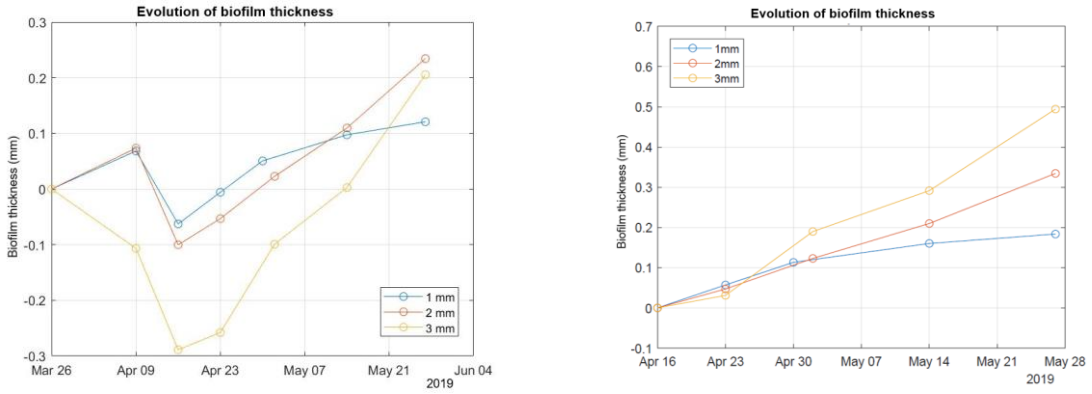

Figure 4.2 – Evolution of biofilm thickness during first stage in two scenarios: zero thickness in 26th March 2019 (Left) and zero thickness in 16th April 2019 (Right)

Considering the evolution of biofilm with a point of origin on the second day, a higher growth of biofilm can be observed. This fact is explained by Figure 4.1 in which a larger unclogged area is observed on 16th April 2019 than on 4th April 2019. Considering that the final unclogged area is the same for both analyses, there will be a larger biofilm growth on the scenario in whose the initial area was greater. Finally, the evolution of biofilm growth

rate is presented below in Figure 4.3, considering 26th March 2019 as zero thickness and 16th April 2019 as zero thickness.

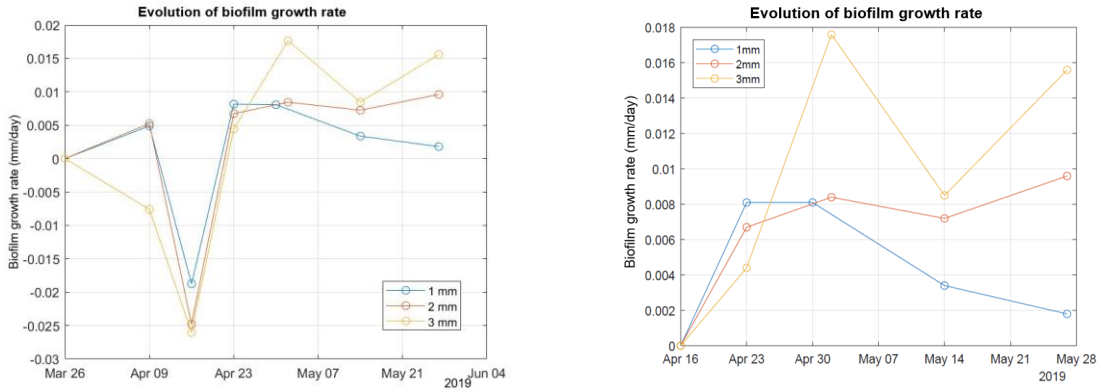

Figure 4.3 - Evolution of biofilm growth rate during first stage in two scenarios: zero thickness in 26th March 2019 (Left) and zero thickness in 16th April 2019 (Right)

It is noted that the values are the same from 23rd March 2019 onwards in both situations. This is not surprising if we consider how this growth rate was calculated by Equations 3.5 and 3.6. The variation in thickness for this calculation is from one day of photography to the next, so it is not important the origin of the analysis, only the variation from one day to the next. From the values presented, it can also be seen that there is no specific behaviour from the growth rate of biofilm between the days regarding the same reactor.

The second stage, which occurred with a flow rate between 0,9 – 1,0 L/h, also presents as the main results the evolution of the average unclogged area, the evolution of the biofilm thickness and the biofilm growth rates in each of the three reactors. Firstly, the evolution of the average unclogged area is observed in Figure 4.4.

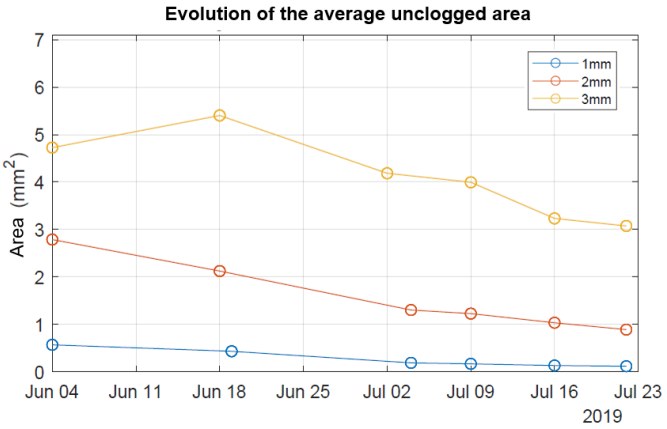

Figure 4.4 - Evolution of the average unclogged area in the second stage

It is noted that there is a slight increase in the unclogged area of reactor 3 from the first to the second observations. Compared to the first stage, it is a much smaller interference, in only one reactor, so when performing the calculations of total biofilm thickness and growth rate, the second stage was not divided into two situations as it was in the previous stage. Therefore, the evolution of the biofilm thickness and the evolution of the growth rate in the second step are presented in Figures 4.5 and Figure 4.6 below.

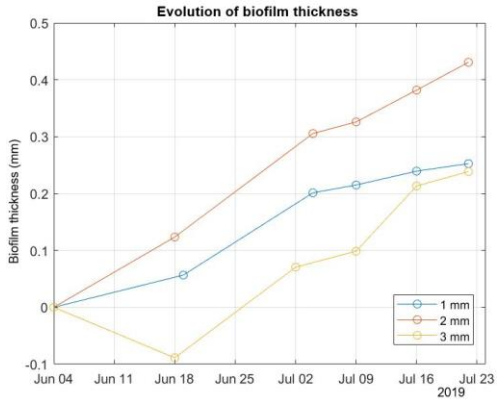

Figure 4.5 - Evolution of biofilm thickness during second stage

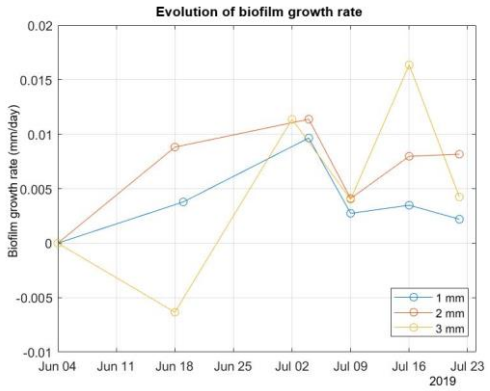

Figure 4.6 - Evolution of biofilm growth rate during second stage

Observing the thickness graph above, the increase of the biofilm thickness with the temporal evolution becomes visible. The reactor 2 was the one with the highest clogging in absolute value. The reactor 3 presents the interference of the decrease of the biofilm thickness on the second day of photography, reaching a negative thickness of approximately -0,1 mm. As said previously, there was a choice not to change the reference of the point of origin because this negative effect was evaluated only in reactor 3 and it is smaller than that which was observed in the first stage, where reactor 3 reaches a negative thickness of approximately -0,3 mm. As observed in the previous step, no specific trend can be observed during the temporal evolution of the growth rate, with moments of increase and decrease in this rate during this period.

5 Discussion

In relation to the first stage of the work, in the analysis of the biofilm clogging it is observed that within the same reactor there is no tendency for greater or lesser development of biofilm in a specific hole of the plate. This observation is explained by the roughness of the surface at the nano and microscales, which influences the adhesion of biofilm to the surface (Malte 1999; Sehar and Iffat 2016). The atypical behaviour of a larger unclogged area after the start of the experiment is derived from a method error, which can be corrected in later practical applications with less variable luminosity for photographs and the insulation of the equipment from sunlight so that there is no interference of natural luminosity on the photographs.

In the analysis starting on 16th April 2019, it is observed that in the first eight days there is a similarity in biofilm thickness in the reactors, which indicates a moment of growth without dependence on pore size. After the eighth day, it was found that the dependence of biofilm growth on pore size exists, which contradicts the assumption of the model proposed by Samsó et al. (2016). In addition to this dependence, it is observed that growth rates do not follow a pattern at any point in the experiment in regard to the temporal evolution, presenting moments of growth rate increase and decrease according to biofilm observations.

In the second stage, the biofilm clogging analyses did not show any tendency for more or less biofilm development in a specific hole or plate, reinforcing the assumption of the influence of surface roughness. The learning with respect to the light conditions influence obtained in the previous stage made it possible that there was no large increase of unclogged area in all reactors in the initial stage. Reactor 3 was the only one which showed an increase of this area resulting in negative thickness, so it was chosen not to divide this step into more scenarios. Because of this choice, it is observed that biofilm developed better at reactor 2, and worse at reactor 3. Regarding

the growth rate, no specific behaviour is observed during the interval, but with similarities between the reactors. The dependence of biofilm growth on pore size is best observed in this second stage where each reactor has a specific thickness evolution behaviour, reinforcing the error of the model assumption proposed by (Samsó et al. 2016).

As a final discussion and the main scope of this work, the two experiences were compared, to understand a little of the influence of the flow in the development of biofilm and clogging. First, to begin the comparison, the experiences of the work were divided into weeks, as shown in Table 5.1 below, to better compare them since the two stages had different durations. For the first stage of the work, the two situations of analysis were considered (different zero day for thickness).

Table 5.1 - Division of work steps into weeks for later comparison

Week	First Stage starts at 26/03/2019	First Stage starts at 16/04/2019	Second Step
1	26/03/2019	16/04/2019	04/06/2019
2	--	23/04/2019	--
3	09/04/2019	30/04/2019 - 02/05/2019	18/06/2019 - 19/06/2019
4	16/04/2019	--	--
5	23/04/2019	14/05/2019	02/07/2019 - 04/07/2019
6	30/04/2019 - 02/05/2019	--	09/07/2019
7	--	27/05/2019	16/07/2019
8	14/05/2019	--	22/07/2019
9	--	--	--
10	27/05/2019	--	--

The comparison was made for the first stage with zero thickness on 16th April 2019 and the second stage in weeks 1, 3, 5 and 7, because the first stage with zero thickness on 26th March 2019 presented negative thickness that are physically impossible, invalidating the results of this stage. In Table 5.2 is the comparison between the first stage (16 th April 2019) and the second stage and in Figure 5.1 is the graphics with the comparison of each reactor with the error bars.

Table 5.2 - Comparison between the first stage (16th April 2019) and the second stage

Week	Average Biofilm thickness (mm)					
	Reactor 1 (1 mm)		Reactor 2 (2 mm)		Reactor 3 (3 mm)	
	First Stage	Second Stage	First Stage	Second Stage	First Stage	Second Stage
1	0,0000	0,0000	0,0000	0,0000	0,0000	0,0000
3	0,1133	0,0566	0,1230	0,1235	0,1898	-0,0888
5	0,1602	0,2013	0,2099	0,3055	0,2916	0,0705
7	0,1836	0,2394	0,3345	0,3818	0,4944	0,2132

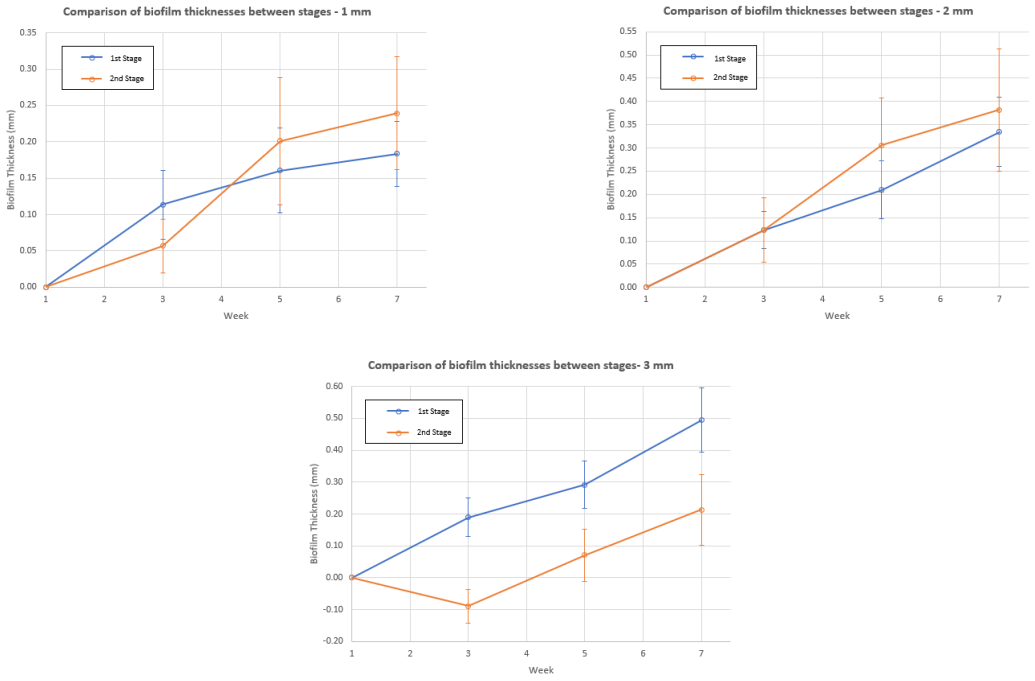

Figure 5.1 – Comparison between first stage (16th April 2019) and second stage: Reactor 1 on left; Reactor 2 on right and Reactor 3 below

In terms of absolute thickness values, it is observed in reactor 1 that in the third week the first stage presented a greater thickness of biofilm than the second stage; however, the situation was reversed and remained until the seventh week with the second stage presenting greater thickness and, consequently, more bioclogging. In the second reactor, a similar thickness is observed between the two stages of the work until the third week. After this period, the second stage showed a higher growth rate until the fifth week that developed the biofilm more. In the end, the thickness of the second stage remained greater, but with little difference from the first stage.

However, these absolute thickness values are derived from averages of all holes in all plates of the same reactor; thus, it is necessary to carry out the analysis considering the standard deviation of these values, which are represented by the vertical error bars. Performing this analysis with the standard deviations, it is noticed that in all weeks of comparison the error bars of the first and second stages overlap, representing that within these average values there is the possibility of situations in which the first stage has thickness of biofilm greater than the second stage or stages have a development of equal thickness of biofilm. Thus, for these two reactors in this work it is not conclusive to state that a lower flow rate (second stage) develops a greater biofilm thickness than a larger flow rate (first stage).

In the comparison of reactor 3, the first stage always presented more thickness than the second stage due to the negative thickness presented on 18th June 2019 (third week) of the second stage. Thus, since the comparison must have results that are physically possible, a new comparison was made considering the zero thickness of reactor 3 on this day. For this, in Table 5.3 below, there is a new week division only for this case, Table 5.4 shows a table of this new comparison and Figure 5.2 shows the graphic with this new comparison and the error bars of each value.

Table 5.3 - New time division of Reactor 3 of the second stage compared to the first stage (16th April 2019)

Week	First Stage (16th April 2019)	Second Stage – 3mm
1	16/04/2019	18/06/2019
2	23/04/2019	--
3	30/04/2019 - 02/05/2019	02/07/2019
4	--	09/07/2019
5	14/05/2019	16/07/2019
6	--	22/07/2019
7	27/05/2019	--

Table 5.4 - Comparison of Reactor 3 in the first step (16th March 2019) and the second step (18th June 2019)

Week	Biofilm thickness (mm) – Reactor 3 (3 mm)	
	First Stage	Second Stage
1	0,0000	0,0000
3	0,1898	0,1593
5	0,2916	0,30202

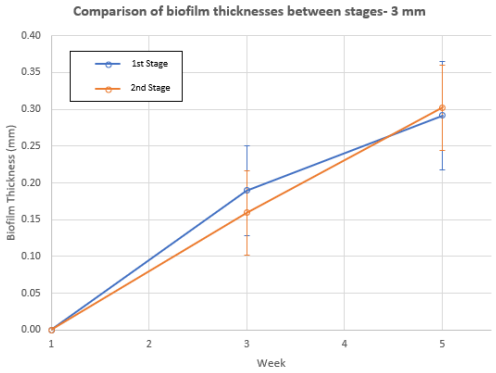

Figure 5.2 – Comparison with Reactor 3 of first stage (16th April 2019) and Reactor 3 of second stage (18th June 2019)

Thus, in this new comparison, a result similar to the one observed earlier is observed, considering that the standard deviations of the values do not conclude whether any stage presents greater biofilm development. In fact, at the end of the five-week comparison, the values of the stages are closer to what was previously observed in the final values of reactor 1 and reactor 2. In general, in all reactors the absolute thickness values of each stage are close in all comparisons and observing the standard deviations of these values in Figures 5.1 and 5.2, it cannot be concluded that any stage, therefore flow rate, has a pattern of developing more biofilm. Comparing the final absolute values of the comparisons of each reactor, it is calculated that the lower flow resulted in thicknesses 30%, 14% and 4% greater than the higher flow, respectively for reactor 1, reactor 2 and reactor 3.

Thus, with the flow rates presented in this work and in the period of time compared, the conclusion is that there is not a clear trend that a flow presents greater biofilm development, resulting in greater pore clogging. The conclusion of this work that there is no greater development of biofilm in any of the flow rates is not compatible with that presented in the literature (Araújo et al. 2016; Liu et al. 2019) about studies with variations in flow rates.

It is necessary to remember that in all works, present and those presented above, only a small range of flow rates and speeds were analyzed and each work with its method. For more solid conclusions regarding the influence of the flow in the development of biofilm, it is essential to carry out more work. Given the small number of studies that relate flow rates to the development of biocolmating, the speed limit or flow rate cannot be determined, as described by (Liu et al. 2019), in which the fluid flow becomes a growth facilitator of biofilm to inhibit its formation. Thus, it is difficult to conclude whether the flow rates of this work are above the limit and, perhaps, that is why the development of thickness was similar in both flow rates of this work.

Taking into account the study by Ostvar et al. (2018), in which of the three flows, the intermediate (0.045 L/h) is the one that presented the highest growth of biofilm and that this flow is lower than that observed in the second

stage of the work, there is a possibility that the flows presented in this work already under the effect of the drag tension. Such possibility should be investigated with later works following the same method.

6 Conclusions

The first conclusion to be made is that the method created by Felício (2018) is valid as a tool for the observation and calculation of biofilm clogging in porous media, but with the necessary attention given to the interference of luminosity in the processing of photographs and the interference of the plate depth.

In the basic levels of statistics, there were no tendencies of biofilm clogging in the holes and plates. However, it was found that there is a dependency between pore size and the growth of biofilm in it. These findings contradict the assumption Samsó et al. (2016) used for one of the most modern mathematical methods simulating the effects of biofilm clogging in ZHC's.

Regarding the comparison of both experiments carried out in this work, it is not possible to conclude whether the flow influences the development of biofilm, which would lead to the pores becoming more clogged. The conclusion is not compatible with the few studies on the issue, but it must be considered that each study was carried out with a range of different flows and with different methods.

References

APHA-AWWA-WPCF. (1995). *Standard Methods for the Examination of Water and Wastewater*. American Public Health/American Water Works Association, Washington, DC.

Araújo, P. A., Malheiro, J., Machado, I., Mergulhão, F., Melo, L., and Simões, M. (2016). "Influence of Flow Velocity on the Characteristics of Pseudomonas fluorescens Biofilms." *Journal of Environmental Engineering*, 1152–1161.

Correia, G. M. P. (2016). "Avaliação da colmatação em leitos de macrófitas." *Dissertação para obtenção do Grau de Mestre em Engenharia do Ambiente, Instituto Superior Técnico, Universidade Técnica de Lisboa*.

Felício, F. G. G. M. L. (2018). "Desenvolvimento de metodologias para a visualização do fenómeno da colmatação em meios poros." *Dissertação para obtenção do Grau de Mestre em Engenharia Civil, Instituto Superior Técnico, Universidade Técnica de Lisboa*.

Kim, J. W., Choi, H., and Pachepsky, Y. A. (2010). "Biofilm morphology as related to the porous media clogging." *Water Research*, Elsevier Ltd, 44(4), 1193–1201.

Liu, N., Skauge, T., Landa-Marbán, D., Hovland, B., Thorbornsen, B., and Radu, F. (2019). "Microfluidic study of effects of flow velocity and nutrient concentration on biofilm accumulation and adhesive strength in the flowing and no-flowing microchannels." *Journal of Industrial Microbiology & Biotechnology*, 46, 855–868.

Malte, H. (1999). "The DLVO theory in microbial adhesion." *Colloids and Surfaces B: Biointerfaces*, 14(1–4), 105–119.

Ostvar, S., Iltis, G., Davit, Y., Schlüter, S., Andersson, L., Wood, B. D., and Wildenschild, D. (2018). "Investigating the influence of flow rate on biofilm growth in three dimensions using microimaging." *Advances in Water Resources*, 117, 1–13.

Samsó, R., García, J., Molle, P., and Forquet, N. (2016). "Modelling bioclogging in variably saturated porous media and the interactions between surface/subsurface flows: Application to Constructed Wetlands." *Journal of Environmental Management*, 165, 271–279.

Sehar, S., and Iffat, N. (2016). "Role of the Biofilms in Wastewater Treatment." *Microbial Biofilms - Importance and Applications*, 25.